Solid State Synthesis and Characterization of Yb^{3+}/Ho^{3+} Doped GdPO$_4$ Nanophosphor for Luminescence Properties

SIRISHA BANDI[1,2,] , MEGHANA ADICHERLA[1,] , GIRIJA VENKATESWARA KONERU[1,] ,
PHANI RAJA KANUPARTHY[1,] and VENKATA NAGENDRA KUMAR PUTTA[1,*,]

[1]Department of Chemistry, GITAM Deemed to be University, Rudraram, Hyderabad-502329, India
[2]Department of Chemistry, B.V. Raju Institute of Technology, Narsapur-502313, India

*Corresponding author: E-mail: pvenkatanagendrakumar@gmail.com; vputta@gitam.edu

A reliable solid-state method for synthesizing GdPO$_4$:Yb^{3+}/Ho^{3+} nanophosphor is presented, exhibiting both up and down conversion luminescent properties. The peaks were observed at 460, 550, 640, and 750 nm after excitation at 300 nm, which is followed by non-radiative resonance energy transfer (ET) with the P-O charge transfer band of Ho^{3+} ions. A significant up-conversion nanophosphors by enhancing Ho^{3+} ion emissions is accomplished. The Ho^{3+} ion peaks at 542 and 635 nm were identified using a strong 980 nm laser source, leading to well-crystalline nanoparticles. The present results demonstrated an enormous potential of GdPO$_4$:Yb^{3+}/Ho^{3+} for high-quality, widespread luminescence. Due to their significant quantum yield when excited at a wavelength of 300 nm, these materials exhibit a diverse array of potential applications and hold considerable potential for advancement across several industries.

Keywords: Solid state method, Nanophosphors, Ytterbium ion, Holmium ion, Gadolinium ion, Photoluminescence.

INTRODUCTION

The fascinating phenomenon of photon up-conversion, commonly referred to as anti-Stokes emission, involves the absorption of infrared photons and the subsequent generation of visible light. The phenomenon under consideration has garnered increasing interest due to its wide array of applications, encompassing but not limited to solar cells, medical devices, temperature sensors, spectrum converters and high-field radiation detection [1]. These applications rely on the use of different rare earths (REs)-doped nanomaterials, which are becoming more and more popular due to their adaptability and simplicity of production. Rare earth orthophosphates are known for their significant chemical and thermal stability, require particular consideration due to their ability to withstand temperatures as high as 1800 ºC. These substances are perfect hosts for numerous applications since they display limited solubility and the necessary optical properties. Furthermore, they are recognized for their capacity to serve as hosts for the containment of radioactive waste [2,3].

In this work, we concentrate on the solid-state method for the synthesis of GdPO$_4$:Yb^{3+}/Ho^{3+} nanoparticles, a dual-mode

nanomaterial. Here, the host matrix for both up-conversion (UC) and down-conversion (DC) luminescence is made up of GdPO$_4$ nanoparticles. Significantly, the modification of the size and morphology of these nanoparticles can be precisely controlled to enhance their luminescent properties when stimulated by a continuous wave laser. This improvement is ascribed to permissive transitions *via* a charge-transfer (CT) process from O^{2-} to Gd^{3+}, which effectively absorbs light between 280 and 300 nm [4,5]. When stimulated at 300 nm, the emission spectra of Ho^{3+} ions under UV light excitation displays discrete peaks at about 460 nm (indirect P-O CTB), 550 nm, 640 nm, and 750 nm. However, in this case, the conversion efficiency is not very high. In order to overcome this restriction, Yb^{3+} is added as a sensitizer, greatly enhance the emission intensity of Ho^{3+} ions throughout the spectrum [6,7]. The Ho^{3+} ions exhibit a highly favourable upconversion luminescent behaviour when subjected to near-infrared light with a wavelength of 980 nm and this characteristic parameter holds a significant potential in a wide range of applications. The current study focuses on the synthesis methodology, characterization of the luminous properties of GdPO$_4$:Yb^{3+}/Ho^{3+} nanophosphors and analyzes

their suitability for applications in surveillance and optical components [8].

EXPERIMENTAL

The chemicals *viz*. ethylene glycol, ammonium dihydrogen phosphate, ytterbium(III) acetate, gadolinium(III) acetate and holmium(III) acetate were of analytical grade reagents and procured from Sigma-Aldrich, USA.

Synthesis of $GdPO_4:Ho^{3+}/Yb^{3+}$ nanoparticles: The solid-state method was adopted to prepare the sample. In this process, 5 mL of conc. HCl was mixed thoroughly with 1.46 g of $Gd(CH_3COO)_3$, 17.4 mg of $Ho(CH_3COO)_3 \cdot xH_2O$ and 356.96 mg of $Yb(CH_3COO)_3 \cdot xH_2O$, 596.56 mg of $(NH_4)_2HPO_4$, 20 mL of ethylene glycol and 5.28 g of NaOH. After that, the mixture were grind in the motor for 4 h by adding acetone to eliminate any leftover HCl. After 4 h of grinding continuously, the samples should be kept for further heating at 150 ºC for atleast 2 h in order to remove volatile matter and get the desired material. Then finally, the prepared material was annealed for 4 h at 900 ºC.

Characterization: The average crystallite size and crystallinity of the synthesized samples were determined using Synchrotron angle-dispersive X-ray diffraction instrument (India). The SEM examination were performed with help of FEI Quanta FEG 250 microscope FEI Company, Hillsboro, USA) equipped with a secondary electron (SE) detector, back-scattered electron (BSE) detector. Using FTIR spectroscopy, the vibrational structure of the generated materials was examined and the up-conversion emission was monitored using a Mono-chromator (iHR322, Horriba Jobin Yvon) containing photo-multiplier tube. A radiation diode laser with a wavelength of 980 nm was employed to induce photoluminescence excitation (PLE) for the upconversion analysis. Beyond UV excitation at 280-300 nm, the downconversion emission spectra of $GdPO_4:Ho^{3+}/Yb^{3+}$ were also studied with a Nd:YAG laser.

RESULTS AND DISCUSSION

XRD studies: The XRD spectrum of the prepared nano-phosphor material $GdPO_4:Ho^{3+}/Yb^{3+}$ co-doped is shown in Fig. 1. The prepared material was annealed for 4 h at high temperature of 900 ºC. The XRD study of the monoclinic phase indicates the existence of strong and powerful diffraction peaks, which indicated the presence defined crystalline structure [9,10]. These diffraction patterns revealed the presence of the monoclinic phase, which is characterized by unequal side lengths and one angle other than 90º. Dopants Yb^{3+} and Ho^{3+} are apparently spread uniformly over the host lattice, as evidenced by the absence of impurity peaks in the XRD pattern. This uniform dispersion is crucial to achieve a consistent and predictable optical properties in the prepared material. The two highest intensity peaks have peak locations, which are near to the diffraction patterns anticipated for the $GdPO_4:Ho^{3+}/Yb^{3+}$ monoclinic structure. According to the theory, this symmetry shows that the co-doped material has a crystal structure very similar to pure $GdPO_4$. The Miller index (011) indicates the presence of extra crystallographic planes in the material. A correlation exists between the orientation of atoms or ions within a crystal
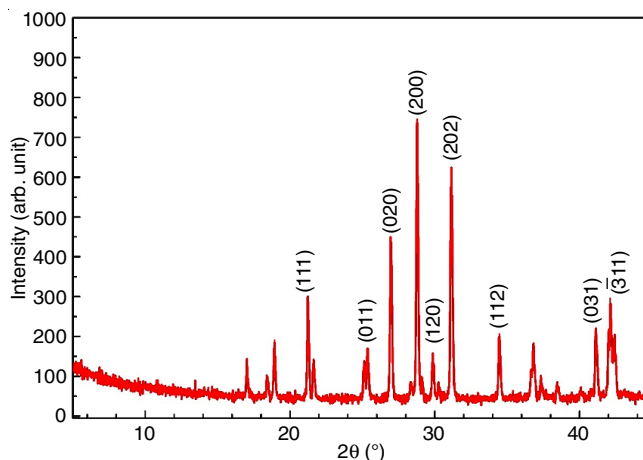

Fig. 1. XRD pattern of $GdPO_4:Ho^{3+}/Yb^{3+}$ samples respectively

lattice and the aforementioned crystallographic planes, namely (020), (200), (120), (202), (112), (031) and ($\overline{3}$11). Each of these planes possesses a distinct orientation within the crystal lattice.

SEM study: The SEM images (Fig. 2) revealed the existence of several different sponge-shaped particles. These sponge like formations appear porous and uneven because of the high-temperature annealing process, which results in distinctive nanostructures. The spherical and sponge-shaped particles have an average size of around 50 nm. Moreover, the images also exhibited the occurrence of different forms, such as conical, cuboid and spherical, in addition to the sponge-shaped particles. Due to the presence of various forms, it is possible that different nanostructures were formed inside the material as a result of the synthesis conditions.

FTIR: The FTIR spectrum of the prepared $GdPO_4:Yb^{3+}/Ho^{3+}$ nanophosphor is shown in Fig. 3. A wide peak at 3400 cm^{-1} is attributed due to the stretching vibrations of the O-H bonds, which implies that the surface of the prepared materials contains hydroxyl (OH) functional groups or water molecules that have been absorbed. A peak at the lower wavenumber 800-600 cm^{-1} is due to the metal-oxygen (M-O) bonds' stret-ching vibrations [11]. In rare earth-doped materials like $GdPO_4:Ho^{3+}/Yb^{3+}$, this region may correspond to the vibrations of the phosphate (PO_4) groups, thereby proving the existence of the host lattice.

Photoluminescence study

Photoluminescence of $GdPO_4:Ho^{3+},Yb^{3+}$

Upconversion (UC) study: Fig. 4 illustrates the UC emission spectra of $GdPO_4$ by Ho^{3+} and Yb^{3+}. The Ho^{3+} doped $GdPO_4$ (Ho^{3+} = 1 at.%) and Yb^{3+} doped $GdPO_4$ (20 at.%) to prepared $GdPO_4:0.01Ho^{3+}/0.2Yb^{3+}$ nanophosphor material. The specific emission wavelength of $GdPO_4:0.01Ho^{3+}/0.2Yb^{3+}$ is dependent on the amount of Ho^{3+} ions and the presence of co-dopants. It has been found that Yb^{3+} ions in this material act as sensitizers [12], also have high efficiency of absorption at 980 nm, the optimal excitation wavelength for the upconversion activities. The absorption co-efficient for Yb^{3+} at 980 nm was found to be 11.601020 cm^2. The green (G) and red (R) emission bands of Ho^{3+} ion are visible at 542 and 650 nm. The detected emi-
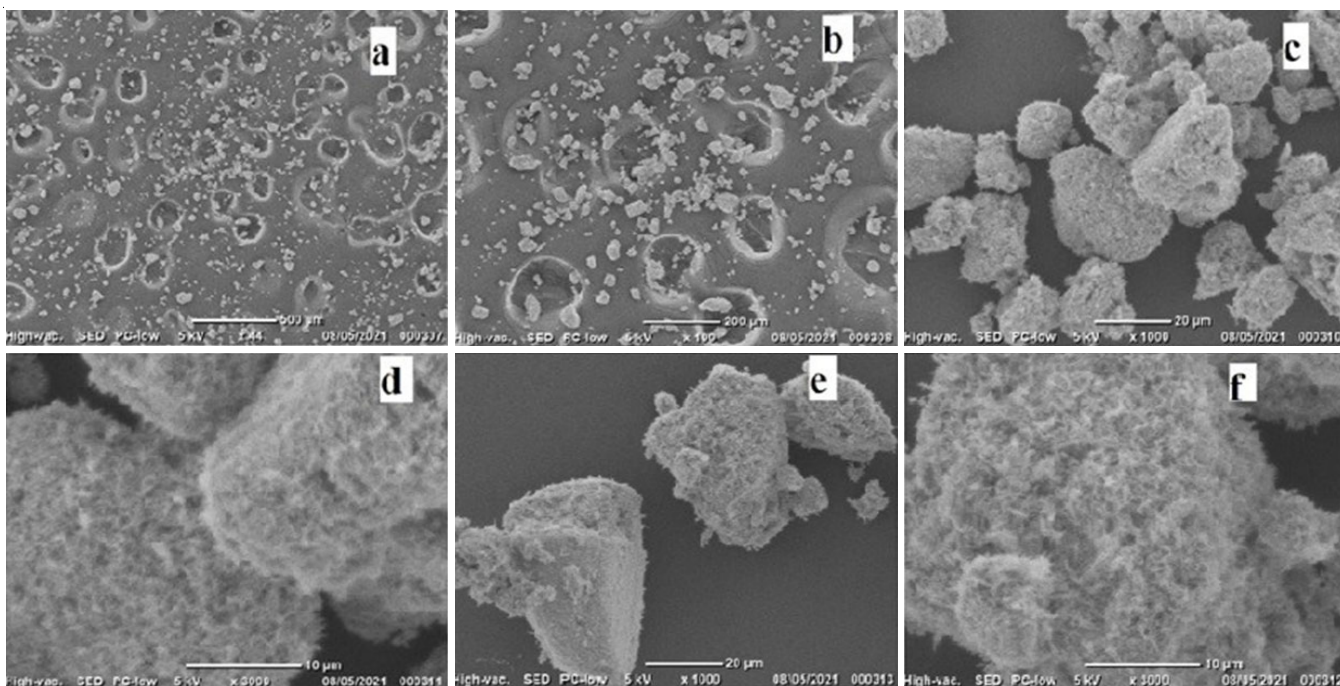
Fig. 2. SEM images of $GdPO_4$:Ho^{3+}/Yb^{3+}
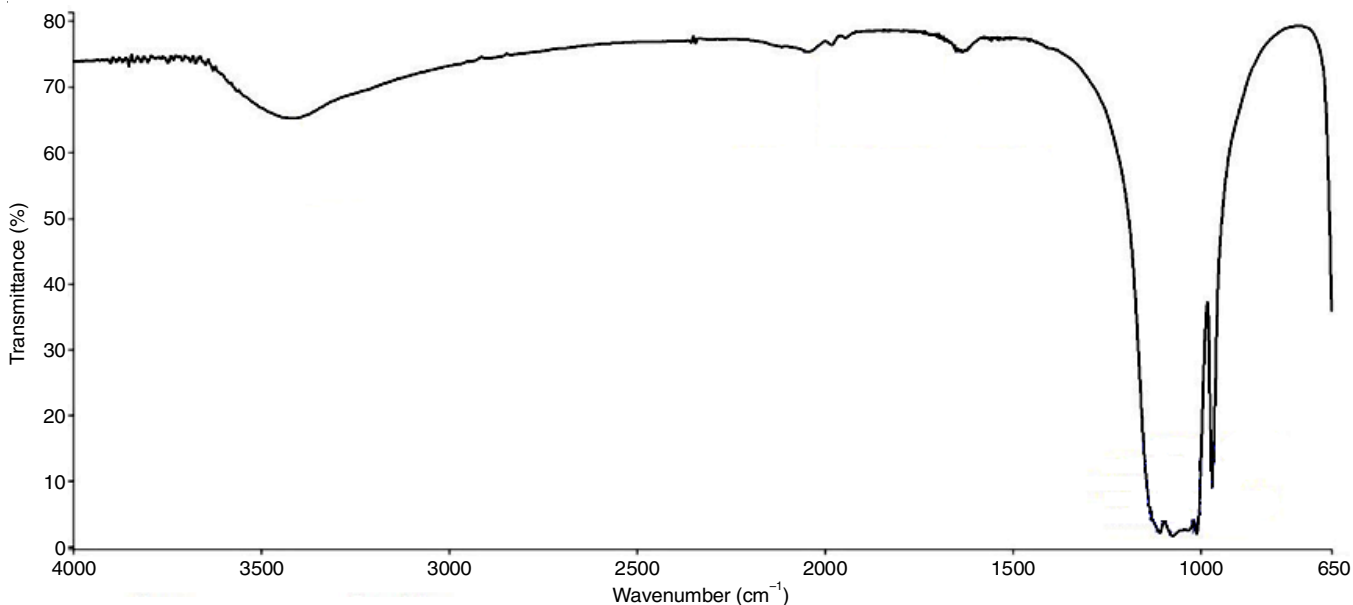
Fig. 3. FT-IR of $GdPO_4$:Ho^{3+}/Yb^{3+}

ssions originate from the electronic transitions initiated by Ho^{3+} ions. Separate emission bands such as characteristic excitation and emission spectra can be observed as a result of these transitions in the upconversion spectrum. The intensity of the unaltered emission changes as a function of the laser input power (P_n) and the number of photons (n) involved in the emission bands [13,14]. Power-dependent changes in the emission properties are demonstrated by an increase in the ratio of red (R) to green (G) emissions (R/G ratio) with increasing laser input power.

Down conversion: When a substance emits light with less energy (lower frequency) than it received results in the Stokes shift. As a result of this shift, low-energy radiant light (E_{em}) is

emitted following excitation (E_{xec}). The downconversion (DC) emission spectrum of the prepared $GdPO_4$:H^{3+}/Yb^{3+} nanophosphor is displayed in Fig. 5. The Ho^{3+} ion energy transfers (ETs) are linked to the distinct emission bands in the DC emission spectra [15,16]. Near-infrared (NIR) (750 nm), red (650 nm) and green (550 nm) light are all emitted during these processes. These emissions originate from the certain electronic transitions in Ho^{3+} ions. It was shown that the $^5F_4$ and $^5S_4 \rightarrow {}^5I_8$ and $^5F_5 \rightarrow {}^5I_8$ ETs of Ho^{3+} correspond to green (550 nm), red (650 nm) and NIR (750 nm) emission bands, respectively. However, the strength of the emission is low. The presence of PO_4^{3-} ions is linked to the observation of a broader emission band (420-520 nm) following excitation at 300 nm. As can be observed
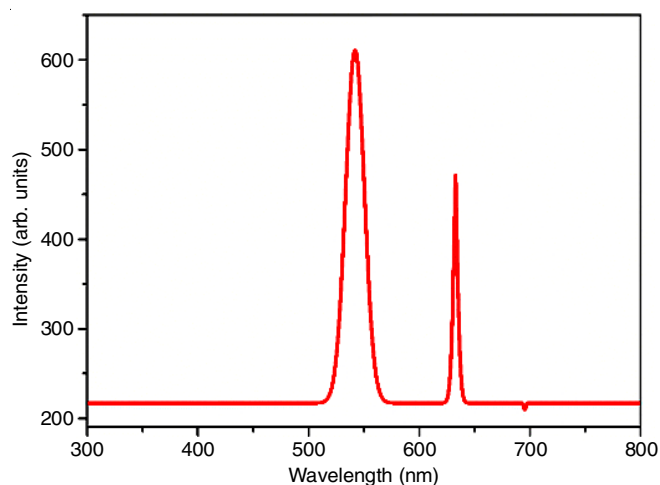
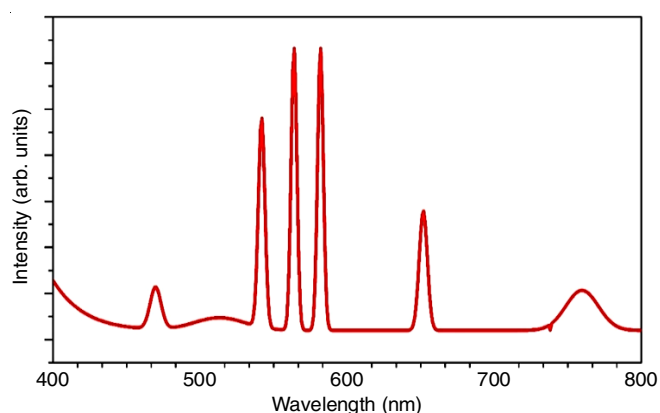Fig. 4. Emission spectra of GdPO$_4$:Ho^{3+}/Yb^{3+}(1 at.%Ho) excited at 980 nm

Fig. 5. Excitation spectrum of GdPO$_4$:Ho^{3+}/Yb^{3+}(1 at.% Ho) excited at 300 nm

from the peaks in the Ho^{3+} emission spectrum, energy has been transferred from the PO$_4^{3-}$ ions to the Ho^{3+} ions. Directly stimulating Ho^{3+} results in the weak emission because of the small absorption of Ho^{3+} ions at 460 nm. The effective excitation of Ho^{3+} and the large absorption at 300 nm are both attributable to resonance energy transfer (ET) from PO$_4^{3-}$ ions to Ho^{3+} ions. The P-O charge transfer band (CTB) transition is associated with the 300 nm peak in the broad region of the spectrum visible from 290 to 360 nm [17,18].

Conclusion

The GdPO$_4$:0.01Ho^{3+}/0.2Yb^{3+} nanophosphor material was successfully synthesized *via* solid-state method. The sample was prepared and annealed at 900 ºC for 4 h to enhance the crystallinity nature. The Ho^{3+} ions in GdPO$_4$:0.01Ho^{3+}/0.2Yb^{3+} demonstrated a substantial upconversion (UC) emission under 980 nm excitation, resulting in the appearance of green and red colour bands at 542 nm ($^5F_4$, $^5S_4 \rightarrow ^5I_8$) and 635 nm ($^5F_5 \rightarrow ^5I_8$), respectively. Along with the conventional Ho^{3+} peaks, 300 nm excitation also produced a wide emission peak at 460 nm, 550 nm, 650 nm and 750 nm ($^5F_4$, $^5S_2 \rightarrow ^5I_7$). Lower conversion rates can be explained by the ligand-to-metal charge transfer (P-O)

band, which is the main cause of the broad emission band. The upconversion study suggests that the green and red bands result from two-photon absorption processes.

CONFLICT OF INTEREST

The authors declare that there is no conflict of interests regarding the publication of this article.

REFERENCES

1. R.S. Perala, R. Joshi, B.P. Singh, V.N.K. Putta, R. Acharya and R.S. Ningthoujam, *ACS Omega*, **6**, 19471 (2021);
https://doi.org/10.1021/acsomega.1c01572

2. Z. Wang, J. Feng, M. Pang, S. Pan and H. Zhang, *Dalton Trans.*, **42**, 12101 (2013);
https://doi.org/10.1039/c3dt51010g

3. Yu. Gao, Y. Qiu, X. Wang, Y. Bi, G. Zhao, F. Ding, Y. Sun and Z. Xu, *RSC Adv.*, **8**, 21857 (2018);
https://doi.org/10.1039/C8RA04198A

4. G.A. Kumar, N.R. Balli, M. Kailasnath, L.C. Mimun, C. Dannangoda, K.S. Martirosyan, C. Santhosh and D.K. Sardar, *J. Alloys Compd.*, **672**, 668 (2016);
https://doi.org/10.1016/j.jallcom.2016.02.165

5. C. Cao, H.K. Yang, B.K. Moon, B.C. Choi and J.H. Jeong, *J. Electrochem. Soc.*, **158**, J6 (2011);
https://doi.org/10.1149/1.3517458

6. J. Hong, F. Liu, M.D. Drami´canin, L. Zhou and M. Wu, *Nanomaterials*, **13**, 1910 (2023);
https://doi.org/10.3390/nano13131910

7. H.-T. Zhu, H.-R. Guo, Q.-J. Zheng, C.-Y. Guan, L.-P. Zhu, H.-B. Li and J.-Y. Yang, *Trans. Nonferrous Met. Soc. China*, **33**, 1205 (2023);
https://doi.org/10.1016/S1003-6326(23)66176-X

8. F. Fiévet, S. Ammar-Merah, R. Brayner, F. Chau, F. Giraud, F. Mammeri, J. Peron, J.-Y. Piquemal, L. Sicard and G. Viau, *Chem. Soc. Rev.*, **47**, 5187 (2018);
https://doi.org/10.1039/C7CS00777A

9. A. Dwivedi, E. Rai, D. Kumar and S.B. Rai, *ACS Omega*, **4**, 6903 (2019);
https://doi.org/10.1021/acsomega.8b03606

10. A. Mahata, K.S. Rawat, I. Choudhuri and B. Pathak, *Sci. Rep.*, **6**, 25590 (2016);
https://doi.org/10.1038/srep25590

11. F. Hu, X. Wei, Y. Qin, S. Jiang, X. Li, S. Zhou, Y. Chen, C.-K. Duan and M. Yin, J. Alloys Compd., **674**, 162 (2016);
https://doi.org/10.1016/j.jallcom.2016.03.040

12. R.S. Perala, B.P. Singh, V.N.K. Putta, R. Acharya and R.S. Ningthoujam, *ACS Omega*, **6**, 19517 (2021);
https://doi.org/10.1021/acsomega.1c01813

13. N. Yaiphaba, R.S. Ningthoujam, N.R. Singh and R.K. Vatsa, *Eur. J. Inorg. Chem.*, 2682 (2010);
https://doi.org/10.1002/ejic.200900968

14. V. Kumar, P. Rani, D. Singh and S. Chawla, *RSC Adv.*, **4**, 36101 (2014);
https://doi.org/10.1039/C4RA04795H

15. W. Ren, G. Tian, L. Zhou, W. Yin, L. Yan, S. Jin, Y. Zu, S. Li, Z. Gu and Y. Zhao, *Nanoscale*, **4**, 3754 (2012);
https://doi.org/10.1039/c2nr30683b

16. C. Cao, Q. Liu, M. Shi, W. Feng and F. Li, *Inorg. Chem.*, **58**, 9351 (2019);
https://doi.org/10.1021/acs.inorgchem.9b01071

17. B. Li, F. Tian, X. Cui, B. Xiang, H. Zhao, H. Zhang, D. Wang, J. Li, X. Wang, X. Fang, M. Qiu and D. Wang, *Nanomaterials*, **12**, 1773 (2022);
https://doi.org/10.3390/nano12101773

18. J. Huang, J. Wu, Y. Chen, X. Gong, Y. Lin, Z. Luo and Y. Huang, *Optical Mater. Expr.*, **12**, 1433 (2022);
https://doi.org/10.1364/OME.451795